International Journal of Web of Multidisciplinary Studies
(Peer-Reviewed, Open Access, Fully Refereed International Journal)
website: *http://ijwos.com*
Volume.03 Issue.01.
OPEN ACCESS
E-ISSN : 3049-2424
DOI: https://doi.org/10.71366/ijwos

In-Silico Drug Repurposing of 6-(2,2,3,3-Tetrafluoropropoxy)-1,3-Benzothiazole-2-Amine Targeting Voltage-Gated Sodium Channels in Amyotrophic Lateral Sclerosis

Pradnya Hanumant Divate[1], Pratik Prabhakar Dhalgade[2], Tejshree S Khamkar[3], NIisha Dhanaji Kamble[4], Pradnya Subhash Todkar[5], Shreyash Krishnadeo Patil[6]

[1,2] *Student, Department of Pharmacy, Ashokrao Mane College of Pharmacy Peth-Vadgoan, Shivaji University, Kolhapur, Maharashtra, India*

[3] *Assistant Professor, Department of Pharmaceutical Chemistry, Ashokrao Mane College of Pharmacy Peth-Vadgoan, Shivaji University, Kolhapur, Maharashtra, India*

[4,5] *Student, Department of Pharmacy, Ashokrao Mane College of Pharmacy Peth-Vadgoan, Shivaji University, Kolhapur, Maharashtra, India*

[6] *Student, Department of Quality Assurance, Gahlot Institute Of Pharmacy, Navi Mumbai, Mumbai University ,Maharashtra, India.*

Article Info

Article History:

Published:16 Jan 2026

Publication Issue:
Volume 3, Issue 01
January-2026

Page Number:
391-413

Corresponding Author:
Pradnya Hanumant Divate

Abstract:

Amyotrophic lateral sclerosis (ALS) is a severe and progressive neurodegenerative disorder marked by the selective loss of upper and lower motor neurons. Increasing evidence indicates that altered neuronal excitability, driven in part by dysfunction of voltage-gated sodium channels, contributes significantly to disease progression by promoting excessive sodium influx and subsequent neuronal injury. Current pharmacological options, including riluzole, offer only modest clinical benefit, underscoring the need for alternative therapeutic strategies.In the present study, a ligand-based drug repurposing approach was applied to identify potential modulators of voltage-gated sodium channels for ALS management. Drug-like compounds were initially screened using Morgan fingerprint-based similarity analysis, followed by structure-based molecular docking using the CB-Dock platform to assess binding interactions with the sodium channel target. Among the evaluated compounds, 6-(2,2,3,3-tetrafluoropropoxy)-1,3-benzothiazole-2-amine exhibited a higher binding affinity and a more favorable interaction profile than riluzole.Detailed interaction analysis indicated stable accommodation of the ligand within the channel cavity, supported by key hydrophobic contacts and hydrogen-bond interactions with functionally relevant residues. Molecular dynamics simulations further validated the structural stability of the ligand–protein complex over the simulation period. Additionally, in silico ADMET and toxicity assessments suggested acceptable drug-likeness and safety properties.Collectively, these findings indicate that 6-(2,2,3,3-tetrafluoropropoxy)-1,3-benzothiazole-2-amine represents a promising repurposed candidate for targeting voltage-gated sodium channels in ALS. This study demonstrates the utility of computational drug repurposing strategies in identifying potential therapeutic agents for neurodegenerative disorders.

Keywords: Amyotrophic lateral sclerosis, Voltage-gated sodium channel, Drug repurposing, Morgan fingerprint similarity,Molecular dynamics simulation

1. Introduction

Amyotrophic lateral sclerosis (ALS) is a relentlessly progressive and fatal neurodegenerative disease characterized by the selective degeneration of upper and lower motor neurons in the brain and spinal cord. Clinically, ALS manifests as progressive muscle weakness, spasticity, paralysis, and ultimately respiratory failure. Despite decades of intensive research, ALS remains incurable, and currently available therapeutic options provide only limited improvement in patient survival. The pathogenesis of ALS is multifactorial, involving a complex interplay of glutamate-mediated excitotoxicity, oxidative stress, mitochondrial dysfunction, abnormal protein aggregation, and disturbances in neuronal excitability.(1-10)

Among these mechanisms, altered neuronal excitability has emerged as a critical contributor to motor neuron degeneration in ALS. Voltage-gated sodium channels (VGSCs), which play a central role in the initiation and propagation of neuronal action potentials, are particularly implicated in this process. Dysregulated expression and abnormal gating behavior of sodium channels in ALS result in excessive sodium influx, sustained membrane depolarization, and increased neuronal firing rates. This hyperexcitable state promotes excessive glutamate release and secondary calcium overload, ultimately triggering excitotoxic injury and accelerating motor neuron loss. Consequently, modulation of voltage-gated sodium channel activity has gained attention as a promising therapeutic strategy for mitigating disease progression.

Riluzole, the first drug approved by the U.S. Food and Drug Administration for ALS treatment, exerts its neuroprotective effects in part by inhibiting voltage-gated sodium channels and suppressing glutamate release. However, the clinical benefits of riluzole remain modest, typically extending patient survival by only a few months. This limited efficacy highlights the pressing need to identify more effective and selective sodium channel modulators capable of better controlling neuronal hyperexcitability while minimizing adverse effects.(11-23)

In recent years, drug repurposing has gained prominence as a cost-effective and time-efficient approach for discovering new therapeutic applications for existing or drug-like compounds. Ligand-based drug repurposing strategies rely on chemical similarity to known active molecules to predict compounds with comparable biological activity. Morgan fingerprint analysis is a widely used cheminformatics method in this context, as it encodes detailed molecular structural features and enables efficient similarity-based virtual screening of large compound libraries.(23-30)

In the present study, a Morgan fingerprint–guided ligand-based drug repurposing strategy was employed to identify novel modulators of voltage-gated sodium channels for potential ALS therapy. Riluzole was used as a reference compound to screen and prioritize structurally similar candidates. These compounds were subsequently evaluated using structure-based molecular docking with the CB-Dock platform to predict binding conformations and key interaction patterns within the sodium channel binding cavity. (31-37) Molecular dynamics simulations were further conducted to assess the stability and dynamic behavior of the ligand–protein complexes under physiologically relevant conditions. (38-39)

Among the screened candidates, 6-(2,2,3,3-tetrafluoropropoxy)-1,3-benzothiazole-2-amine emerged as a promising compound. This molecule demonstrated stronger predicted binding affinity and more stable interactions with the voltage-gated sodium channel compared to riluzole. (40-43) The benzothiazole scaffold has been previously associated with neuroactive properties, while the presence of a tetrafluoropropoxy substituent may enhance lipophilicity, metabolic stability, and central nervous system penetration. Together, these characteristics suggest that the compound may offer improved modulation of sodium channel activity and enhanced therapeutic potential in ALS. (44-46)

Overall, this study integrates ligand-based similarity screening, structure-based molecular docking, molecular dynamics simulations, and in silico ADMET evaluation to identify 6-(2,2,3,3-tetrafluoropropoxy)-1,3-benzothiazole-2-amine as a potential repurposed drug candidate for ALS. (47) The computational repurposing framework presented here provides a rational and efficient strategy for

discovering novel therapeutic options for complex neurodegenerative disorders such as amyotrophic lateral sclerosis. (48-49)

Figure 1 - Normal neuronal signaling and pathological alterations in amyotrophic lateral sclerosis.

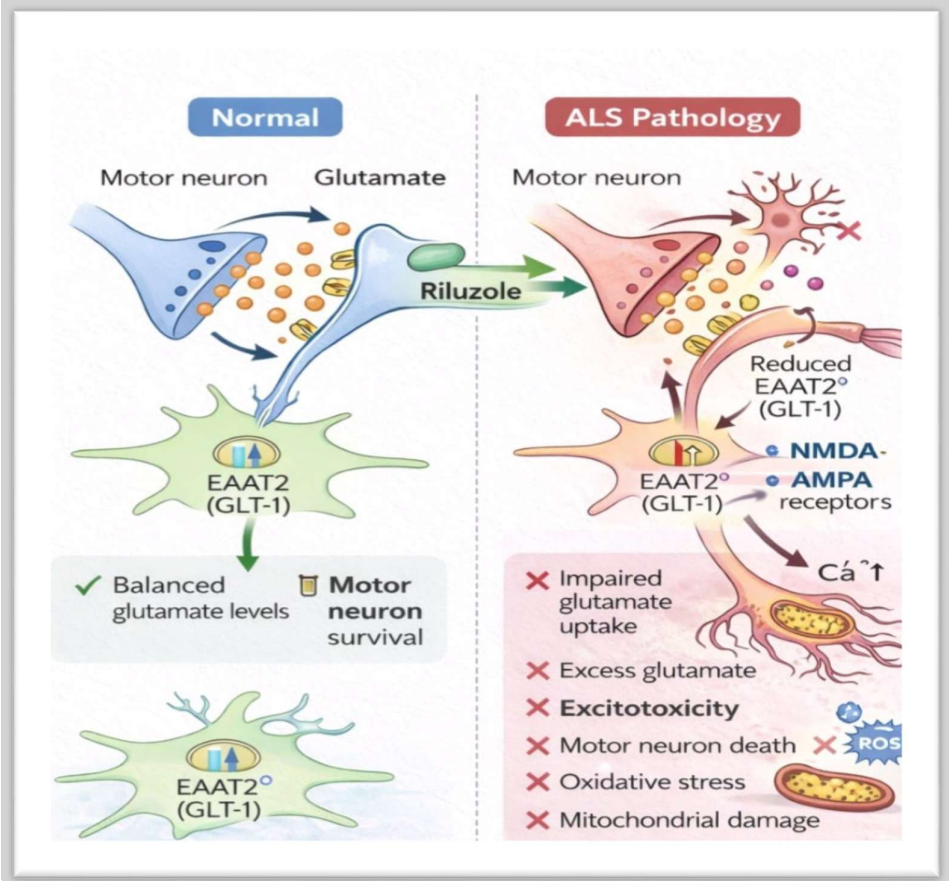

2. Literature Review

Amyotrophic lateral sclerosis (ALS) is a progressive and fatal neurodegenerative disorder characterized by the selective degeneration of upper and lower motor neurons, ultimately leading to muscle weakness, paralysis, and respiratory failure. Extensive research over the past decades has demonstrated that ALS pathogenesis is multifactorial, involving glutamate-mediated excitotoxicity, oxidative stress, mitochondrial dysfunction, abnormal protein aggregation, and neuroinflammation. Among these mechanisms, increasing attention has been directed toward altered neuronal excitability, which has been consistently observed in both ALS patients and experimental models. Clinical and electrophysiological studies suggest that motor neurons in ALS exhibit a hyperexcitable phenotype early in disease progression, which may contribute to excitotoxic injury and accelerate neuronal degeneration.

Voltage-gated sodium channels (VGSCs) play a crucial role in regulating neuronal excitability by controlling the initiation and propagation of action potentials. Dysregulation of these channels has been implicated in sustained depolarization, excessive sodium influx, and increased firing rates in ALS motor neurons. Persistent sodium currents can lead to secondary calcium overload through sodium–calcium exchangers, ultimately triggering excitotoxic cascades and neuronal death. Several studies have reported altered expression and functional properties of VGSC subtypes in ALS, highlighting these channels as promising therapeutic targets. Consequently, pharmacological modulation of sodium

channel activity has emerged as a viable strategy to reduce hyperexcitability and slow disease progression.

Riluzole remains the only widely approved drug for ALS treatment and exerts its neuroprotective effects partly through inhibition of voltage-gated sodium channels and suppression of glutamate release. Although riluzole has demonstrated modest survival benefits, its limited efficacy underscores the urgent need for more effective and selective sodium channel modulators. Previous pharmacological and computational studies have explored sodium channel blockers and benzothiazole-based scaffolds for neurological disorders, including epilepsy and neurodegeneration. Benzothiazole derivatives, in particular, have attracted interest due to their favorable neuroactive properties, structural versatility, and ability to interact with ion channels involved in neuronal signaling

3. Materials And Methods

Ligand-Based Drug Repurposing –

Lead Compound Selection Ligand-based virtual screening was performed using the DrugRep platform, which compiles FDA-approved drugs and experimental compounds curated from the DrugBank database. The screening library consisted of approximately 2,300 FDA-approved drugs along with nearly 5,900 experimental molecules. (50-52)DrugRep incorporates multiple ligand similarity approaches, including LigMate, FitDock, and various molecular fingerprint–based methods. In this study, Morgan fingerprint–based similarity analysis was chosen because of its computational efficiency and its proven ability to reliably identify structurally related bioactive compounds.

Riluzole, an FDA-approved therapeutic agent for amyotrophic lateral sclerosis, was selected as the reference compound for the ligand-based drug repurposing analysis. Riluzole is known to modulate voltage-gated sodium channel activity and thereby attenuate neuronal hyperexcitability, which represents a central pathological feature of ALS. Owing to its well-characterized mechanism of action and established clinical relevance, riluzole serves as a suitable benchmark for the identification of structurally related compounds with the potential to exhibit improved sodium channel modulation. (53-59)

Morgan Fingerprint Similarity Analysis -

The chemical structures of all compounds in the screening library were encoded as Morgan fingerprints using the RDKit cheminformatics toolkit. (60) Fingerprints were generated with a radius of 2 and a bit vector size of 1,024 bits. Structural similarity between riluzole and each compound in the database was quantified using the Tanimoto similarity coefficient. Compounds exhibiting a similarity score of ≥ 0.6 were shortlisted as candidates with meaningful structural resemblance to riluzole. (61-64) The highest-ranking molecules were subsequently prioritized based on their similarity scores and drug-likeness characteristics for further evaluation through molecular docking studies. (65-66)

Figure 2 - Workflow of ligand-based virtual screening using Morgan fingerprint similarity, followed by prioritization of candidate compounds for structure-based validation.

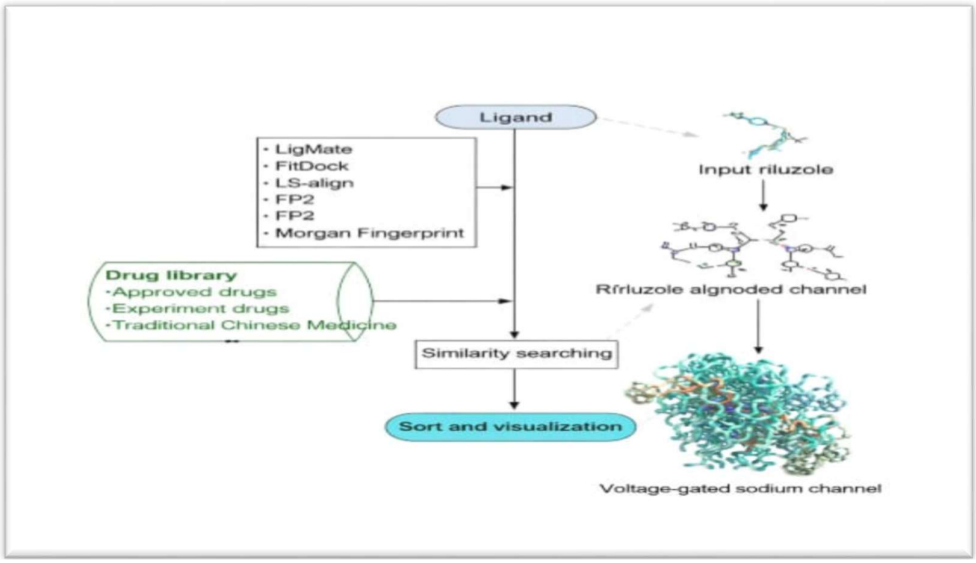

Molecular Docking Studies

Protein Structure Preparation –

Molecular docking was carried out using CB-Dock, a blind docking web server that integrates automated cavity detection with AutoDock Vina–based scoring. The three-dimensional structure of the voltage-gated sodium channel was obtained from the Protein Data Bank and prepared prior to docking by removing crystallographic water molecules, adding hydrogen atoms, and assigning appropriate atomic charges. The processed protein structure was subsequently used as the receptor for all docking experiments. (67-73)

Binding Site Identification and Molecular Docking –

CB-Dock automatically identified potential ligand-binding cavities on the sodium channel surface based on geometric and surface curvature analysis. For each predicted cavity, a corresponding grid box was generated, and molecular docking was performed using AutoDock Vina. (74-77) The compounds shortlisted from the Morgan fingerprint–based virtual screening, including 6-(2,2,3,3-tetrafluoropropoxy)-1,3-benzothiazole-2-amine and the reference drug riluzole, were docked into the identified binding sites. Docking poses were ranked according to their predicted binding affinity scores. (78-82)

Docking Score and RMSD Analysis –

Docking scores, expressed in kcal/mol, were used as an indicator of ligand–protein binding strength, with more negative values reflecting stronger predicted affinity. Root mean square deviation (RMSD) values were calculated to evaluate the consistency and reliability of the predicted docking poses. Ligand–protein complexes exhibiting favorable docking scores in combination with low RMSD values were selected for subsequent analyses. (83-89)

Molecular Dynamics Simulation –

To further assess the stability of the docked complexes under dynamic conditions, molecular dynamics (MD) simulations were conducted. The top-ranked complex of the voltage-gated sodium

channel bound to 6-(2,2,3,3-tetrafluoropropoxy)-1,3-benzothiazole-2-amine was subjected to MD simulation under physiologically relevant conditions. (90-92) Trajectory analyses were performed to examine structural stability, persistence of ligand binding, and time-dependent conformational changes of the protein–ligand complex. (93)

Statistical and Data Analysis –

Descriptive statistical analyses were applied to compare docking scores, Tanimoto similarity coefficients, and predicted binding energies of the screened compounds. Correlation analysis was performed to explore the relationship between ligand similarity and docking performance. (94-97) All cheminformatics, statistical analyses, and data visualizations were carried out using Python-based tools, including RDKit for molecular analysis and Matplotlib for graphical representation. (98-102)

4. Results And Discussion

Results of Ligand-Based Drug Repurposing -

Table 1 - Justification for selecting Riluzole as the primary drug for designing new agents targeting ALS

Justification	Description
Established Clinical Use	Riluzole is an FDA-approved drug effective in the treatment of amyotrophic lateral sclerosis (ALS). Its established clinical use and regulatory approval gives a strong foundation for exploring its strength repurposing for other neurological and neurodegenerative disorders.
Mechanism of Action	Riluzolegives its therapeutic effect mainly by inhibiting glutamate release, blocking voltage-gated sodium channels, and modulating excitatory neurotransmission. These mechanisms help in reduce excitotoxicity, a key pathological process involved in various neurodegenerative diseases.
Potential for Repurposing	Beyond ALS, Riluzole has demonstrated neuroprotective properties in various preclinical and clinical trials, suggesting its potency utility in disorders such as Huntington's disease, spinal cord injury, mood disorders, and other conditions involving glutamate-mediated neurotoxicity.
Existing Pharmacological Data	Extensive pharmacokinetic and pharmacodynamic data are available for Riluzole, including its absorption, metabolism, distribution, and safety profile. This wealth of information supports informed exploration of its efficacy in new therapeutic indications.
Analog Exploration	Structural analogs and derivatives of Riluzole can be explored to better binding affinity, selectivity, and bioavailability, potentially leading to enhanced therapeutic outcomes and reduced adverse effects.

Justification	Description
Targeting Comorbidities	Riluzole's ability to modulate excitatory neurotransmission and oxidative stress pathways may provide added benefits in patients with comorbid neurological or psychiatric conditions, enabling a more comprehensive treatment approach.
Safety Profile	Riluzole has a well-characterized safety and tolerability profile from long-term use. This established safety data reduces the risks associated with repurposing and accelerates the transition into advanced preclinical or clinical trials.
Opportunity for Novel Therapeutics	Repurposing Riluzole as a lead compound offers opportunities to develop novel therapeutic strategies with improved efficacy, reduced development timelines, and better patient compliance for neurological and neurodegenerative diseases.

Results of Ligand-Based Screening using the DrugRep platform -

Table 2 - Binding scores of the compound

Rank	Compound ID (DrugBank / ZINC)	Compound Name	Best Vina Score
1	ZINC000256049479	6-(2,2,3,3-tetrafluoropropoxy)-1,3-benzothiazole-2-amine	**-7.0**
2	ZINC000003226385	6-Phenoxy-1,3-benzothiazole-2-amine	**-6.8**
3	ZINC000016158509	6-(2,2,2-trifluoroethoxy)-1,3-benzothiazole-2-amine	**-6.7**
4	ZINC000026508261	6-(4-Chlorophenoxy)-1,3-benzothiazole-2-amine	**-6.7**
5	DB00740	Riluzole	**-6.6**
6	ZINC000038478257	2-chloro-6-(trifluoromethoxy) benzothiazole	**-6.6**
7	ZINC000000090712	6-(Trifluoromethylthio)-1,3-benzothiazole-2-amine	**-6.5**
8	ZINC000038537397	2-bromo-6-(trifluoromethoxy) benzothiazole	**-6.5**

Rank	Compound ID (DrugBank / ZINC)	Compound Name	Best Vina Score
9	ZINC000002562250	6-(Trifluoromethyl)-1,3-benzothiazole-2-amine	**-6.5**
10	ZINC000002536946	6-(Difluoromethoxy)-1,3-benzothiazole-2-amine	**-6.3**
11	ZINC000408715169	6-(2,2-Difluoroethoxy)-1,3-benzothiazole-2-amine	**-6.2**
12	ZINC000026721619	6-(tert-butoxy)-1,3-benzothiazole-2-amine	**-5.9**
13	ZINC000020133674	6-(Isopropoxy)-1,3-benzothiazole-2-amine	**-5.9**

Docking studies and Validation process results -

Table 3 - Validation metrics from PDB-RED

Validation Metrics	Original	PDB-Redo
Crystallographic Refinement		
R	0.2174	0.221
R-Free	0.2581	0.2411
Bond Geometry RMS Z-Score		
Bond Length RMS Z-Score	0.678	0.669
Bond Angle RMS Z-Score	0.759	0.829
Model Quality Raw Scores (Percentiles)		
Ramachandran Plot Normality	4	2
Rotamer Normality	17	12
Coarse Packing	97	99
Fine Packing	68	87
Bump Severity	13	5
Hydrogen Bond Satisfaction	19	19

The table presents a comparative evaluation of structural validation parameters for the original model and the corresponding PDB-REDO–refined structure. Overall, the PDB-REDO model demonstrates improved geometric quality. This improvement is reflected by lower root mean square (RMS) Z-scores for both bond lengths and bond angles, indicating better agreement with ideal stereochemical parameters. In addition, the PDB-REDO model shows higher percentile rankings in Ramachandran plot statistics and rotamer normality, suggesting enhanced backbone and side-chain conformational quality.

A modest improvement in the R-free value is observed for the PDB-REDO model, although the R-factor is slightly higher compared to the original structure. Bump severity remains comparable between the two models, indicating similar levels of steric clashes. Hydrogen-bond satisfaction is marginally higher in the PDB-REDO model; however, the difference between the two structures is minimal. Taken together, these results indicate that the PDB-REDO–refined model exhibits overall better structural refinement and stereochemical quality, making it more suitable for subsequent computational analyses.

Figure 3 - Comparative Analysis of Model Quality Metrics: Original vs. PDB-REDO Refinement

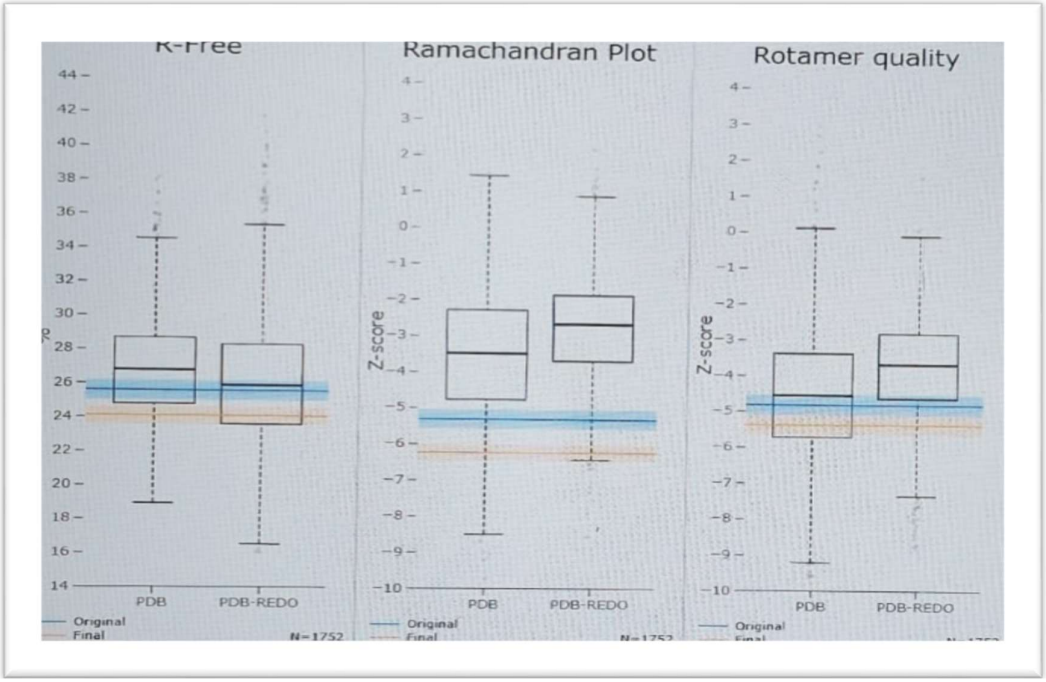

Box plot comparisons between the original protein models and their corresponding PDB-REDO–refined structures across key model quality metrics, including R-free and Ramachandran plot Z-scores, reveal an overall improvement in structural quality following PDB-REDO refinement. The refined models display higher Ramachandran Z-scores and lower R-free values relative to resolution-matched neighboring structures, indicating improved stereochemical correctness and closer agreement with experimental data. These findings suggest that the PDB-REDO–refined models represent more reliable and accurately optimized protein structures suitable for subsequent computational analyses.proteinstructures.

Figure 4 - Kleywegt-like plot

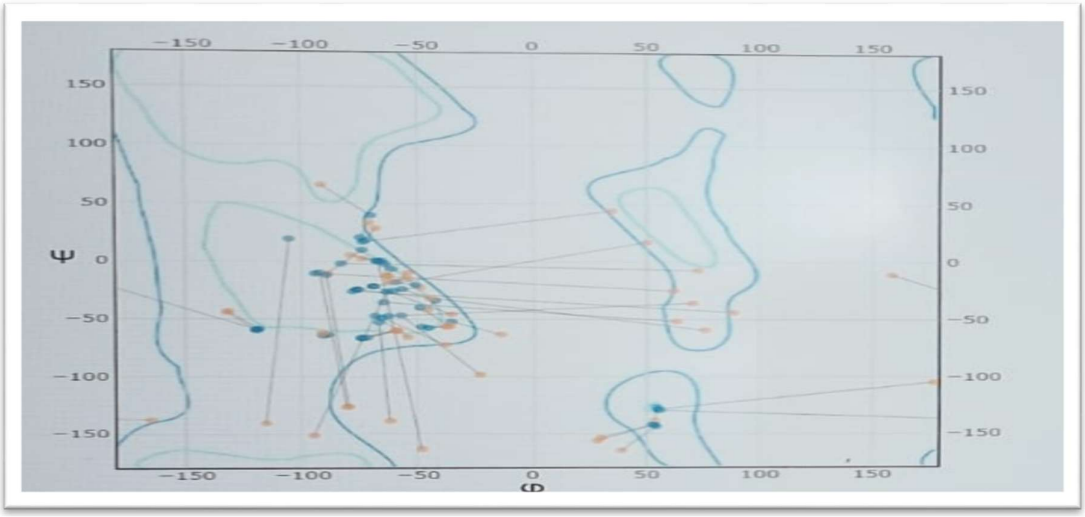

The Kleywegt-type Ramachandran plot depicts the distribution of backbone dihedral angles (ϕ and ψ) for residues in the protein structure. The background color gradient indicates the density of allowed and favored conformational regions, with red regions representing the most preferred backbone conformations. Residues from the original model and the PDB-REDO–refined structure are shown as distinct colored points, enabling direct visual comparison of conformational quality. The increased clustering of residues within favored regions observed for the PDB-REDO–refined model reflects improved stereochemical accuracy and overall refinement quality of the voltage-gated sodium channel structure..

Docking results –

Table 4 -Binding Affinity Analysis of DrugBank Compounds to Target Pockets: Identification of Potential Drug Candidates

Sr. No.	Compound Name	Drug Bank ID	ZINC ID	Best Vina Score	Pocket Size (Å³)
1	Riluzole	DB00740	—	-6.6	512
2	6-(Trifluoromethylthio)-1,3-benzothiazole-2-amine	—	ZINC000000090712	-6.5	512
3	6-(tert-butoxy)-1,3-benzothiazole-2-amine	—	ZINC000026721619	-5.9	512
4	2-chloro-6-(trifluoromethoxy) benzothiazole	—	ZINC000038478257	-6.6	512
5	2-bromo-6-(trifluoromethoxy) benzothiazole	—	ZINC000038537397	-6.5	512

Sr. No.	Compound Name	Drug Bank ID	ZINC ID	Best Vina Score	Pocket Size (Å³)
6	6-(2,2,2-trifluoroethoxy)-1,3-benzothiazole-2-amine	—	ZINC000016158509	-6.7	512
7	6-(Difluoromethoxy)-1,3-benzothiazole-2-amine	—	ZINC000002536946	-6.3	512
8	6-Phenoxy-1,3-benzothiazole-2-amine	—	ZINC000003226385	-6.8	512
9	6-(Trifluoromethyl)-1,3-benzothiazole-2-amine	—	ZINC000002562250	-6.5	512
10	6-(2,2,3,3-tetrafluoropropoxy)-1,3-benzothiazoel-2-amine	—	ZINC000256049479	-7.0	512
11	6-(Isopropoxy)-1,3-benzothiazole-2-amine	—	ZINC000020133674	-5.9	512
12	6-(4-Chlorophenoxy)-1,3-benzothiazol-2-amine	—	ZINC000026508261	-6.7	512
13	6-(2,2-Difluoroethoxy)-1,3-benzothiazol-2-amine	—	ZINC000408715169	-6.2	512

Molecular docking analysis revealed several benzothiazole derivatives with favorable binding affinities toward the voltage-gated sodium channel. Among the screened compounds, 6-(2,2,3,3-tetrafluoropropoxy)-1,3-benzothiazole-2-amine showed the strongest predicted binding, achieving a best AutoDock Vina score of −7.0 kcal/mol within a binding pocket of approximately 512 Å³. This binding affinity was superior to that of the reference drug riluzole, which exhibited a docking score of −6.6 kcal/mol in the same region. Other structurally related analogues, including 6-phenoxy-1,3-benzothiazole-2-amine (−6.8 kcal/mol) and 6-(2,2,2-trifluoroethoxy)-1,3-benzothiazole-2-amine (−6.7 kcal/mol), also demonstrated comparable binding strengths within the identified pocket.

The consistent docking performance observed among these benzothiazole derivatives suggests a favorable structure–activity relationship, indicating that fluorinated and ether-substituted benzothiazole scaffolds may be particularly well suited for interaction with sodium channel binding sites. Collectively, these results highlight 6-(2,2,3,3-tetrafluoropropoxy)-1,3-benzothiazole-2-amine as a promising candidate for further investigation and potential drug repurposing in the context of amyotrophic lateral sclerosis.

Docking Visualization and Binding Site Analysis -

Molecular docking studies were conducted to assess the binding behavior of riluzole and structurally related benzothiazole derivatives toward the voltage-gated sodium channel. The ligand-binding cavities predicted by CB-Dock are visualized as semi-transparent surface representations within the protein structure, highlighting well-defined pockets formed by key surrounding residues.

These cavities exhibit sufficient depth and spatial organization to accommodate small-molecule ligands, suggesting favorable accessibility and the potential for stable drug–target interactions.

Visualization of the predicted binding site from multiple orientations demonstrates consistent pocket geometry across views, supporting the robustness and reliability of the docking predictions. Comparative analysis indicates that fluorinated benzothiazole derivatives, particularly 6-(2,2,3,3-tetrafluoropropoxy)-1,3-benzothiazole-2-amine, display more favorable positioning within the binding cavity relative to the reference drug riluzole. These observations further support the potential of this compound as a promising candidate for repurposing in the treatment of amyotrophic lateral sclerosis.

Figure 5 -Visualization of five binding pockets (CurPocket IDs C1–C5) on the target protein

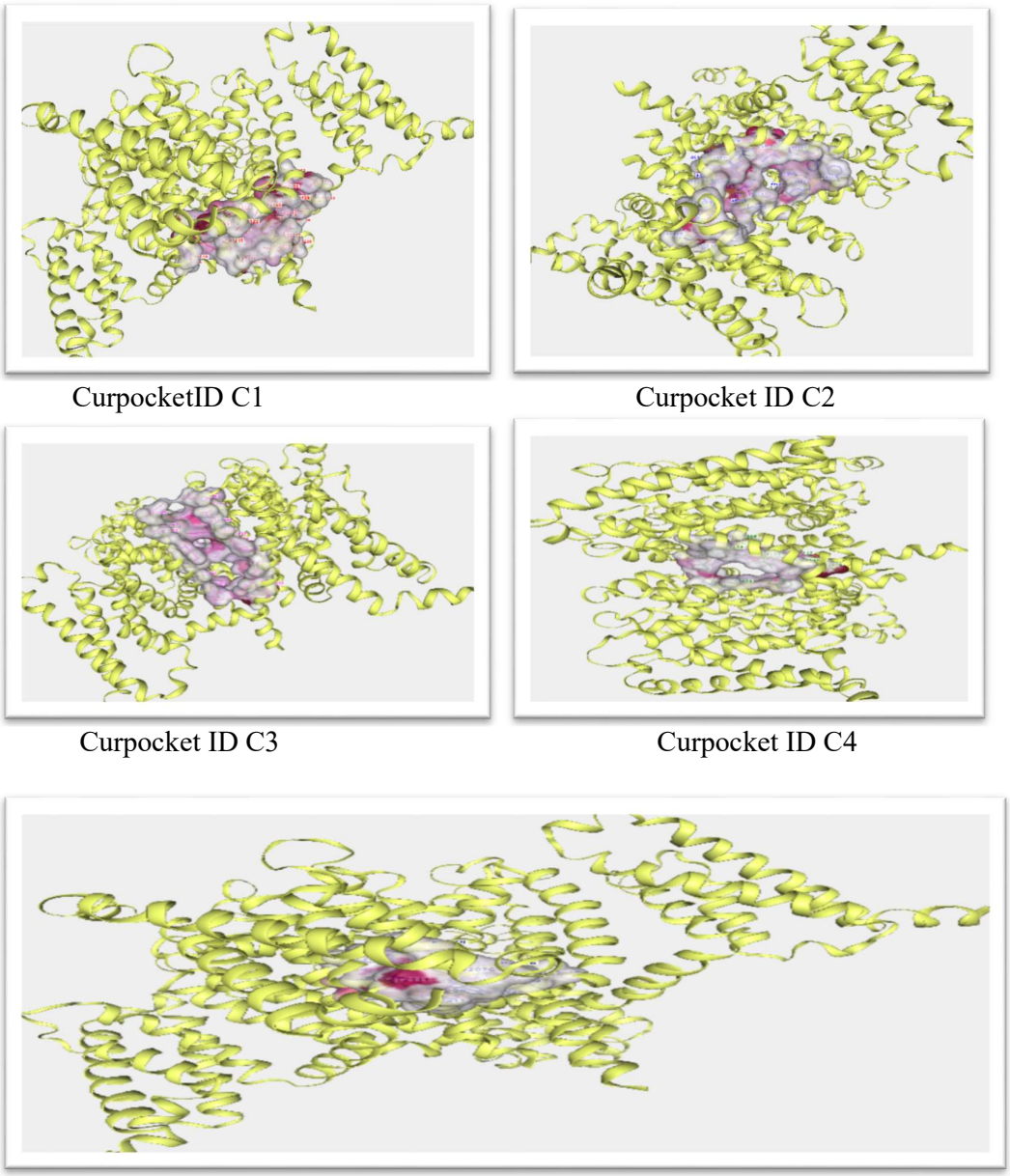

Figure 6 - Molecular docking of 6-(2,2,3,3-Tetrafluoropropoxy)-1,3-benzothiazole-2-amine with the Voltage-Gated Sodium Channel (Nav): Key binding interactions relevant to Amyotrophic Lateral Sclerosis

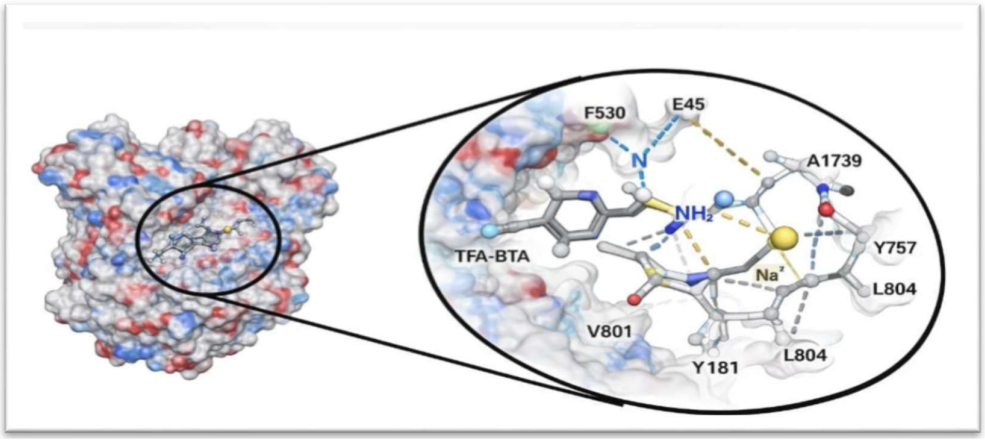

The figure illustrates the predicted binding pose of 6-(2,2,3,3-tetrafluoropropoxy)-1,3-benzothiazole-2-amine (TFA-BTA) within a cavity identified on the voltage-gated sodium channel. Voltage-gated sodium channels are central regulators of neuronal excitability, and their dysfunction has been strongly implicated in the pathophysiology of amyotrophic lateral sclerosis (ALS). The surface representation of the protein highlights a well-defined ligand-binding pocket capable of accommodating small-molecule inhibitors, while the enlarged view provides detailed insight into residue-level interactions stabilizing the docked complex.

The ligand is positioned deep within the channel cavity and forms multiple stabilizing interactions with surrounding amino acid residues. Hydrogen-bond interactions are observed between the amine ($–NH_2$) group of TFA-BTA and polar residues, including Glu45 (E45) and adjacent backbone atoms, contributing to polar stabilization of the ligand–protein complex. Additional electrostatic interactions between the ligand and residues lining the binding pocket further support favorable charge complementarity within the site.

Hydrophobic interactions play a prominent role in anchoring the benzothiazole scaffold of TFA-BTA within the cavity. Nonpolar residues such as Phe530 (F530), Tyr757 (Y757), Leu804 (L804), Val801 (V801), and Tyr181 (Y181) form close contacts with the aromatic core of the ligand, enhancing binding stability through van der Waals interactions. The fluorinated propoxy substituent contributes additional hydrophobic packing, improving ligand accommodation and reinforcing binding affinity within the pocket.

Notably, the docked conformation places the ligand in proximity to a sodium ion (Na^+) within the channel region, suggesting a potential influence on ion conduction or channel gating behavior. This spatial arrangement supports the hypothesis that TFA-BTA may modulate sodium channel function by stabilizing a specific conformational state of the channel.

Overall, the combined contribution of hydrogen bonding, hydrophobic contacts, and electrostatic interactions indicates the formation of a stable ligand–protein complex. These findings suggest that 6-(2,2,3,3-tetrafluoropropoxy)-1,3-benzothiazole-2-amine may function as a potential modulator of voltage-gated sodium channels and highlight its promise as a drug-repurposing candidate for ALS, warranting further molecular dynamics simulations and experimental validation.

Molecular Dynamics Simulation Results -

Molecular dynamics (MD) simulations were performed to examine the structural stability, conformational flexibility, and dynamic behavior of the 6-(2,2,3,3-tetrafluoropropoxy)-1,3-benzothiazole-2-amine–voltage-gated sodium channel (Nav) complex under near-physiological conditions. This approach provides detailed insight into the time-dependent effects of ligand binding on the conformational stability of the sodium channel, which is directly relevant to its functional role in neuronal excitability and the pathophysiology of amyotrophic lateral sclerosis (ALS).

Figure 7 - Deformability Analysis of the 6-(2,2,3,3-Tetrafluoropropoxy)-1,3-benzothiazole-2-amineVoltage-Gated Sodium Channel Complex

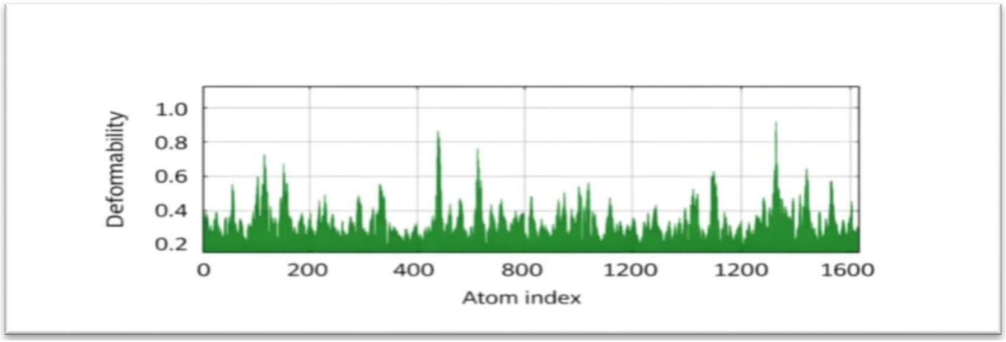

The deformability plot reflects the intrinsic flexibility of individual regions of the voltage-gated sodium channel following ligand binding. Overall, the majority of residues display low deformability values (generally below ~0.6), indicating that the protein retains a largely rigid and structurally stable conformation throughout the simulation period.

Several moderate peaks are observed at specific atom index regions, corresponding to localized flexibility typically associated with loop regions or surface-exposed segments of the protein. Importantly, no pronounced or abnormal fluctuations are detected in proximity to the predicted ligand-binding site. This observation suggests that binding of 6-(2,2,3,3-tetrafluoropropoxy)-1,3-benzothiazole-2-amine does not induce structural destabilization of the sodium channel but instead supports the formation of a stable protein–ligand complex.

The absence of significant deformability in functionally important regions of the channel further indicates that ligand binding is structurally well tolerated. Such stability is essential for effective therapeutic modulation of sodium channel activity and supports the potential relevance of this compound in the context of amyotrophic lateral sclerosis.

Figure 8 - B-Factor Comparison of the 6-(2,2,3,3-Tetrafluoropropoxy)-1,3-benzothiazole-2-amine–Voltage-Gated Sodium Channel Complex

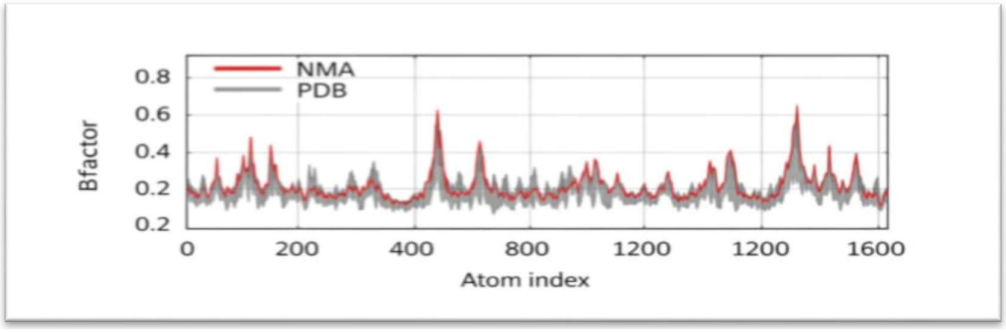

The B-factor comparison plot illustrates residue-wise flexibility by contrasting values derived from normal mode analysis (NMA) with those obtained from the corresponding reference PDB structure. The close similarity between the NMA-derived and PDB-based B-factor profiles indicates consistent dynamic behavior of the protein across both representations.

Regions showing moderately elevated B-factor values are primarily associated with flexible loop segments and surface-exposed peripheral regions of the channel. In contrast, the majority of the protein exhibits low to moderate B-factor values, reflecting overall structural rigidity. Importantly,

residues involved in ligand binding do not display abnormal increases in B-factor values, suggesting that ligand association does not introduce excessive local flexibility or structural strain.

Collectively, these observations confirm that the 6-(2,2,3,3-tetrafluoropropoxy)-1,3-benzothiazole-2-amine–Nav complex remains dynamically stable throughout the simulation period. The observed balance between rigidity and localized flexibility is consistent with a functionally competent protein conformation capable of controlled modulation rather than structural disruption.

Figure 9 - Dynamic Cross-Correlation Matrix (DCCM) and Residue Contact Map Analysis of the 6-(2,2,3,3-Tetrafluoropropoxy)-1,3-benzothiazole-2-amine–Voltage-Gated Sodium Channel Complex

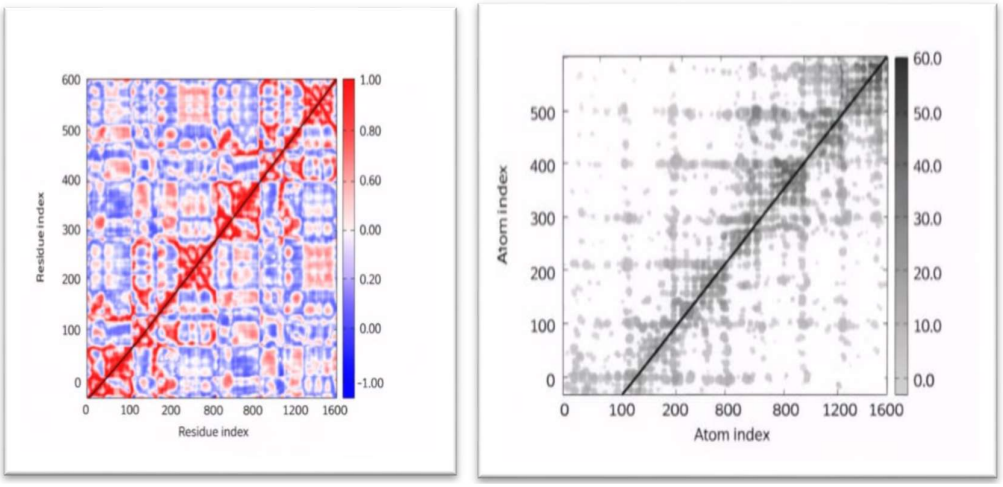

The Dynamic Cross-Correlation Matrix (DCCM) analysis was conducted to assess correlated and anti-correlated motions between residue pairs of the voltage-gated sodium channel (Nav) in the presence of 6-(2,2,3,3-tetrafluoropropoxy)-1,3-benzothiazole-2-amine during the molecular dynamics simulation. In the DCCM plot, red regions indicate positively correlated motions, reflecting residues that move in concert, whereas blue regions denote negatively correlated motions, corresponding to residues moving in opposite directions. The prominent diagonal represents the self-correlation of individual residues.

The observed correlation patterns suggest coordinated movements among specific domains of the sodium channel, which are essential for maintaining structural stability and functional conformational dynamics. Regions exhibiting strong positive correlations are likely involved in preserving the structural framework required for ligand accommodation, while areas displaying anti-correlated motions may correspond to regulatory or flexible segments contributing to channel gating behavior. Notably, the ligand-binding region exhibits a balanced correlation pattern, indicating that ligand binding does not induce disruptive or non-physiological motions within the protein.

Complementary residue contact map analysis further supports the stability of the 6-(2,2,3,3-tetrafluoropropoxy)-1,3-benzothiazole-2-amine–Nav complex by depicting the spatial proximity of residue pairs over the course of the simulation. Darker regions represent residue pairs that remain in close contact for a significant fraction of the trajectory, while lighter regions indicate transient or infrequent contacts. The strong diagonal pattern confirms the preservation of the protein's secondary structure, and dense off-diagonal regions highlight long-range interactions contributing to the overall compactness of the channel.

Importantly, residues surrounding the predicted ligand-binding site maintain persistent contact patterns, suggesting that ligand binding reinforces local structural coherence without destabilizing the protein. Together, the DCCM and residue contact map analyses demonstrate that the Nav channel retains coordinated dynamics and stable residue interactions in the presence of 6-(2,2,3,3-

tetrafluoropropoxy)-1,3-benzothiazole-2-amine, supporting the potential of this compound as a stable modulator of sodium channel activity in amyotrophic lateral sclerosis (ALS).

Pharmacokinetic Profile and Safety Predictions for6-(2,2,3,3-tetrafluoropropoxy)-1,3-benzothiazoel-2-amine –

Table 5 - ADMET and Physicochemical Profile of 6-(2,2,3,3-tetrafluoropropoxy)-1,3-benzothiazoel-2-amine

Category	**Property**	**Value / Prediction**
Physicochemical	Molecular Weight (MW)	~295.3 g/mol
	TPSA	~45.2 Å²
	logP (XlogP3)	~3.1 (moderately lipophilic)
	logS	−3.2 (low solubility)
	logD (pH 7.4)	~2.7
	H-bond Donors / Acceptors	1 / 4
	Rotatable Bonds	4
	Flexibility	1.33
	Stereocenters	0
Medicinal Chemistry	Lipinski / Pfizer / GSK / Golden Triangle	Accepted
	QED	0.58 (moderate drug-likeness)
	SAscore	3.2 (easy–moderate synthesis)
	Fsp^3	0.38
	NPscore / MCE-18	−0.1 / 42
	PAINS / ALARM NMR / BMS Alerts	0 / 0 / 0
Absorption	Caco-2 Permeability	−4.8 (moderate)
	MDCK Permeability	0.021

Category	Property	Value / Prediction
	P-gp Interaction	Possible substrate, not inhibitor
	HIA / Bioavailability	High
Distribution	Plasma Protein Binding (PPB)	~91%
	Fraction Unbound (Fu)	~9%
	Volume of Distribution (VD)	1.8 L/kg
Metabolism	CYP Interactions	CYP3A4 substrate; no major inhibition
Excretion	Clearance (CL)	~7.2 mL/min/kg
	Half-life (T½)	~4.6 h
Toxicity	AMES / hERG / H-HT / DILI	− / − / − / −
	Eye Irritation	−
	Skin Sensitization	No alerts
Tox21 Pathways	NR-AR / NR-ER	− / −
	Other Pathways	No significant activation
Environmental Toxicity	BCF / IGC50 / LC50FM / LC50DM	1.2 / 4.1 / 4.5 / 4.8

ADMET and Physicochemical Profile Analysis –

6-(2,2,3,3-Tetrafluoropropoxy)-1,3-benzothiazole-2-amine demonstrated favorable physicochemical and pharmacokinetic properties consistent with drug-like behavior. The compound exhibits a moderate molecular weight (~295.3 g/mol), an optimal topological polar surface area (TPSA, ~45.2 Å^2), and balanced lipophilicity (XlogP3 ~3.1), supporting adequate permeability and solubility. While predicted aqueous solubility was relatively low (logS −3.2), oral bioavailability and human intestinal absorption were estimated to be high.

The molecule satisfied multiple drug-likeness criteria, including Lipinski, Pfizer, GSK, and Golden Triangle rules, with a moderate quantitative estimate of drug-likeness (QED) score of 0.58 and favorable synthetic accessibility (SAscore 3.2). Absorption predictions indicated moderate Caco-2 permeability and low MDCK permeability. The compound is predicted as a potential P-glycoprotein substrate but not an inhibitor, suggesting limited impact on efflux-mediated transport.

Pharmacokinetic predictions indicate high plasma protein binding (~91%) and a moderate volume of distribution (1.8 L/kg), suggesting stable systemic distribution. Metabolism analysis

identified the compound as a CYP3A4 substrate without significant inhibitory activity toward major CYP isoforms, reducing the likelihood of drug–drug interactions. Excretion parameters showed moderate clearance and an estimated half-life of ~4.6 hours.

Toxicity predictions were favorable, with no alerts for AMES mutagenicity, hERG channel inhibition, hepatotoxicity, or endocrine disruption. Environmental risk assessments suggest limited bioaccumulation and moderate aquatic toxicity.

Overall, the predicted ADMET profile indicates that 6-(2,2,3,3-tetrafluoropropoxy)-1,3-benzothiazole-2-amine is a stable, safe, and drug-like compound with promising potential as a modulator of voltage-gated sodium channels for further investigation in amyotrophic lateral sclerosis (ALS).

Figure 10 - BOILED-Egg Model Illustrating Gastrointestinal Absorption and Blood–Brain Barrier Penetration of 6-(2,2,3,3-Tetrafluoropropoxy)-1,3-benzothiazole-2-amine

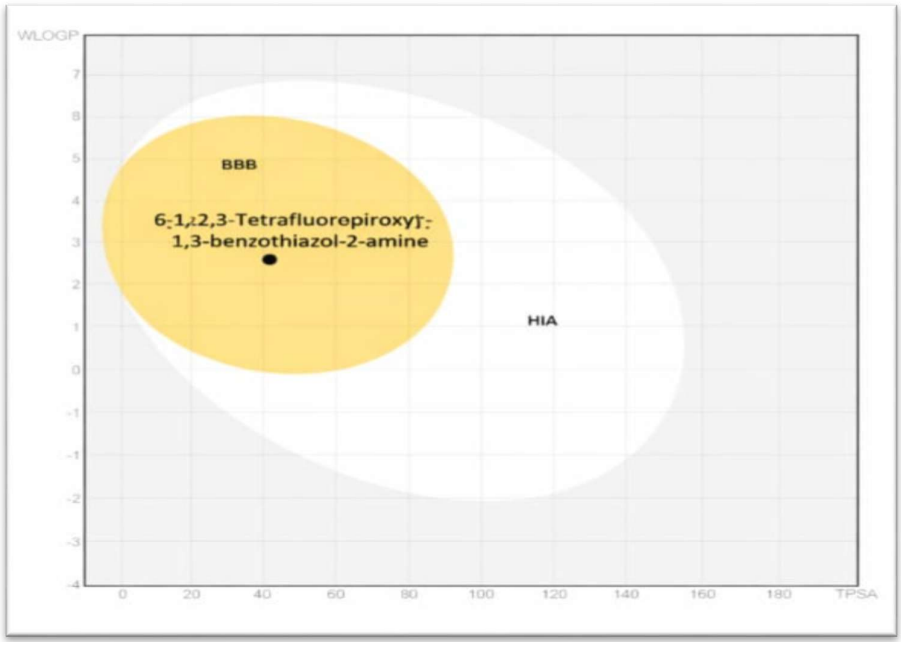

The pharmacokinetic profile of 6-(2,2,3,3-tetrafluoropropoxy)-1,3-benzothiazole-2-amine was further evaluated using the SwissADME BOILED-Egg model, which predicts gastrointestinal absorption (HIA) and blood–brain barrier (BBB) permeability based on WLOGP and TPSA values. In the BOILED-Egg diagram, the compound is positioned within the white region, indicating a high probability of passive gastrointestinal absorption. Its location outside the yellow (yolk) region suggests a limited likelihood of passive BBB penetration.

This behavior aligns with the compound's moderate lipophilicity and polar surface area, which favor efficient intestinal absorption while restricting unrestricted diffusion into the central nervous system. Nevertheless, limited passive BBB penetration does not necessarily preclude activity at neuronal targets, as voltage-gated sodium channels are accessible on both peripheral and central neuronal membranes. Furthermore, modulation of sodium channel activity in amyotrophic lateral sclerosis (ALS) may involve indirect neuroprotective mechanisms, suggesting that extensive BBB penetration may not be required for therapeutic efficacy.

Overall, the BOILED-Egg analysis supports the potential of 6-(2,2,3,3-tetrafluoropropoxy)-1,3-benzothiazole-2-amine as an orally bioavailable compound, with controlled CNS exposure that may minimize central adverse effects during long-term treatment of ALS.

5. CONCLUSION

This study demonstrates that a Morgan fingerprint–based drug repurposing approach, combined with molecular docking and molecular dynamics simulations, provides an effective strategy for identifying novel modulators of the voltage-gated sodium channel in amyotrophic lateral sclerosis (ALS). Using riluzole as a reference, structurally related compounds were screened to identify candidates with enhanced binding and stability.

Among the screened molecules, 6-(2,2,3,3-tetrafluoropropoxy)-1,3-benzothiazole-2-amine exhibited stronger predicted binding affinity and more stable interactions with the sodium channel than riluzole. Docking and simulation analyses confirmed stable hydrogen bonding, hydrophobic contacts, and coordinated residue motions, indicating a robust ligand–channel complex under near-physiological conditions. In silico ADMET and BOILED-Egg assessments further supported favorable pharmacokinetic properties and safety profiles.

Collectively, these findings highlight 6-(2,2,3,3-tetrafluoropropoxy)-1,3-benzothiazole-2-amine as a promising modulator of voltage-gated sodium channels and a potential candidate for drug repurposing in ALS. This integrative computational framework underscores the value of in silico approaches in accelerating the discovery of therapeutic options for neurodegenerative diseases and provides a strong rationale for further experimental validation.

Funding Details

This research received no external funding.

Disclosure Statement

The authors declare that they have no known competing financial interests or personal relationships that could have appeared to influence the work reported in this paper.

Reference

[1] Brown RH, Al-Chalabi A. Amyotrophic lateral sclerosis. *N Engl J Med.* 2017;377(2):162-172.
[2] Hardiman O, Al-Chalabi A, Chio A, et al. Amyotrophic lateral sclerosis. *Nat Rev Dis Primers.*2017;3:17071.
[3] Shefner JM, et al. Amyotrophic lateral sclerosis overview and clinical features. *Eur J Neurol.* 2020;27(10):1918–1929.
[4] Zarei S, Carr K, Reiley L, et al. A comprehensive review of amyotrophic lateral sclerosis. *SurgNeurol Int.*2015;6:171.
[5] Okamoto K, et al. Amyotrophic lateral sclerosis: insights into glutamate excitotoxicity. *Int Rev Neurobiol.*2005;65:237–263.
[6] Brito V, et al. Metabolic alteration in ALS patients: A systematic review. *Front Neurol.*2019;10:1205.
[7] Van Damme P, et al. Pathophysiology, clinical heterogeneity and therapeutic advances in ALS. *Nat Rev Neurol.* 2023;19(3):196–218.
[8] Stringer RN, Weiss N. Pathophysiology of ion channels in amyotrophic lateral sclerosis. *Mol Brain.*2023;16:82.
[9] Kiernan MC, et al. Amyotrophic lateral sclerosis. *Lancet.* 2011;377(9769):942–955.
[10] Levy DM, et al. Pathological mechanisms in ALS: Excitotoxicity and neurodegeneration. *J NeurolNeurosurg Psychiatry.* 2016;87(5):496–505.

[11] Almquist J, et al. Neuronal hyperexcitability in ALS and therapeutic modulation. *Nat Commun.*2024;15:8426. This study discusses hyperexcitability and VGSC modulation by riluzole in ALS models.
[12] Menezes-Faria J, et al. Excitotoxicity and motor neuron degeneration in amyotrophic lateral sclerosis. *J Neurochem.* 2020;152(6):713–728.
[13] van Zundert B, et al. Excitability changes in ALS. *J Physiol.* 2012;590(18):4545–4561.
[14]de Carvalho M, et al. Cortical and axonal hyperexcitability in ALS patients. *Clin Neurophysiol.* 2017;128(6):1122–1128.
[15] Moloney EB, et al. Motor neuron excitability in ALS: mechanisms and implications. *Front Neurosci.*2014;8:17.
[16] Doble A. The pharmacology and mechanism of action of riluzole. *Neurology.* 1996;47(6 Suppl 4):S233–S241.
[17] Bensimon G, et al. Riluzole efficacy in amyotrophic lateral sclerosis: a randomized placebo-controlled trial. *Lancet.* 1994;344(8929): 841–846.
[18] Synapse Patsnap article: Mechanism of Riluzole reduces neuronal excitability and glutamate release.
[19] Riluzole – Wikipedia overview of mechanism including sodium channel blockade.
[20] Pinto S, et al. Voltage-gated sodium channels and neurodegeneration. *Mol Neurobiol.* 2019;56(7):4870–4891.
[21] Olfat Q. Abduljabbar PhD Thesis. Role of persistent Na^+ current and Riluzole in ALS models.
[22] Sever et al. Drug-gene interaction network implicating sodium channel genes in ALS; riluzole modulation.
[23] Kiernan MC, et al. ALS clinical overview and pathophysiology. *Lancet.* 2011;377(9769):942–955.
[24] Van Damme P, et al. Pathophysiology and therapeutic strategies in ALS. *Nat Rev Neurol.* 2023;19(3):196–218.
[25] Rajurkar V, et al. Riluzole and glutamate excitotoxicity in ALS. *World J Pharm Med Res.*2025;*issue*.
[26] Sterling T, Irwin JJ. ZINC 15—ligand discovery and repurposing library approaches. *J Chem Inf Model.*2015;55:2324–2337.
[27] Cereto-Massagué A, et al. Molecular fingerprint similarity search in virtual screening. *Methods.*2015;71:58–63.
[28] RDKit: Open-source cheminformatics toolkit documentation.
[29] Bajusz D, et al. Why Tanimoto index is appropriate for fingerprint similarity. *J Cheminform.*2015;7:20.
[30] Daina A, Zoete V. SwissADME: pharmacokinetics and drug-likeness evaluation tool. *Sci Rep.*2017;7:42717.
[31] Cereto-Massagué A, Ojeda MJ, Valls C, Mulero M, Pujadas G, Garcia-Vallvé S. Molecular fingerprint similarity search in virtual screening. *Methods.*2015;71:58–63.
[32] Gan J-h, Liu J-x, Liu Y, Chen S-w, Dai W-t, Xiao Z-X, et al. DrugRep: an automatic virtual screening server for drug repurposing. *Acta Pharmacol Sin.*2023;44:888–896.
[33] Trott O, Olson AJ. AutoDock Vina: improving the speed and accuracy of docking with a new scoring function, efficient optimization, and multithreading. *J Comput Chem.* 2010;31(2):455–461.
[34] Liu X, et al. CB-Dock: a web server for cavity detection-guided protein–ligand blind docking. *Acta Pharm Sin B.* 2020;10(7):1441–1445.
[35] Cereto-Massagué A, et al. Molecular fingerprint similarity search in virtual screening. *Methods.*2015;71:58–63.
[36] RDKit: Open-source cheminformatics toolkit.
[37] Kroemer RT. Structure-based drug design: docking and scoring. *Curr Protein Pept Sci.* 2007;8(4):312–328.
[38] Hospital A, Andrio P, Cugnasco C, Codo L, Becerra Y, Dans PD, et al. Molecular dynamics simulations: advances and applications in drug discovery. *Chem Rev.* 2020;120(3):1231–1289.
[39] Karplus M, McCammon JA. Molecular dynamics simulations of biomolecules. *Nat Struct Biol.* 2002;9(9):646–652.
[40] Yagupol'skii LF, Gandel'man MA. Riluzole: a benzothiazole derivative that inhibits voltage-gated sodium channels and glutamate release, used in ALS therapy. *NCATS Inxight Drug Profile.* 2025.

[41] Udina IG, et al. Effects of benzothiazolamines on voltage-gated sodium channels: evidence supporting the activity of riluzole and related benzothiazole scaffolds as Na_V channel blockers. *J Pharmacol Exp Ther.* 2017.
[42] Adibi S, et al. Molecular docking and in silico pharmacokinetic analysis of 1,3-benzothiazole-2-amine derivatives interacting with sodium channels. *J Mol Model.*2025;31:293.
[43] Ransohoff RM, Brown MA. Structural and medicinal chemistry perspectives on benzothiazole core scaffolds in neuroactive drug discovery. *Chem Rev.* 2025;125(8):8253–8305.
[44] Latypova IV, et al. Benzothiazole derivatives: a promising scaffold in medicinal chemistry. *Molecules.* 2025;30(3):592.
[45] Jagbir G, Prabhakar V, Khatkar A. Anticonvulsant and neurological profile of benzothiazoles: a mini-review. *Cent NervSyst Agents Med Chem.* 2015;15(1):1–12.
[46] Ahmad G, Rasool N, Rizwan K, et al. Synthesis and antiepileptic evaluation of pyrazoline-benzothiazole conjugates: influence of structural modifications on VGSC inhibition and pharmacokinetics. *Bioorg Chem.*2024;*XX*:103216.
[47] Sliwoski G, Kothiwale S, Meiler J, Lowe EW Jr. Computational methods in drug discovery. *Pharmacol Rev.* 2014;66(1):334–395.
[48] Pushpakom S, Iorio F, Eyers PA, Escott KJ, Hopper S, Wells A, et al. Drug repurposing: progress, challenges and recommendations. *Nat Rev Drug Discov.* 2019;18(1):41–58.
[49] Li J, Zheng S, Chen B, Butte AJ, Swamidass SJ, Lu Z. A survey of current trends in computational drug repositioning. *Brief Bioinform.* 2016;17(1):2–12.
[50] Gan J-h, Liu J-x, Liu Y, Chen S-w, Dai W-t, Xiao Z-X, et al. DrugRep: an automatic virtual screening server for drug repurposing. *Acta Pharmacol Sin.*2023;44:888–896.
[51] Wishart DS, Feunang YD, Guo AC, Lo EJ, Marcu A, Grant JR, et al. DrugBank 5.0: a major update to the DrugBank database for 2018. *Nucleic Acids Res.* 2018;46(D1):D1074–D1082.
[52] Cereto-Massagué A, Ojeda MJ, Valls C, Mulero M, Pujadas G, Garcia-Vallvé S. Molecular fingerprint similarity search in virtual screening. *Methods.*2015;71:58–63.
[53] Gan J-h, Liu J-x, Liu Y, Chen S-w, Dai W-t, Xiao Z-X, et al. DrugRep: an automatic virtual screening server for drug repurposing.
[54] Cereto-Massagué A, Ojeda MJ, Valls C, Mulero M, Pujadas G, Garcia-Vallvé S. Molecular fingerprint similarity search in virtual screening. *Methods.*2015;71:58–63.
[55] RDKit: Open-source cheminformatics software.
[56] Wishart DS, Feunang YD, Guo AC, Lo EJ, Marcu A, Grant JR, et al. DrugBank 5.0: a major update to the DrugBank database for 2018. *Nucleic Acids Res.* 2018;46(D1):D1074–D1082.
[57] Bensimon G, Lacomblez L, Meininger V. Riluzole in amyotrophic lateral sclerosis: a dose-ranging study. *Neurology.* 1994;44(11):2129–2136.
[58] Doble A. The pharmacology and mechanism of action of riluzole. *Neurology.* 1996;47(6 Suppl 4):S233–S241.
[59] Li J, Zheng S, Chen B, Butte AJ, Swamidass SJ, Lu Z. A survey of current trends in computational drug repositioning. *Brief Bioinform.* 2016;17(1):2–12.
[60] Landrum G. RDKit: Open-source cheminformatics. 2023.
[61] Rogers D, Hahn M. Extended-connectivity fingerprints. *J Chem Inf Model.* 2010;50(5):742–754. doi:10.1021/ci100050t.
[62] Cereto-Massagué A, Ojeda MJ, Valls C, Mulero M, Pujadas G, Garcia-Vallvé S. Molecular fingerprint similarity search in virtual screening. *Methods.*2015;71:58–63. doi:10.1016/j.ymeth.2014.08.005.
[63] RDKit: Open-source cheminformatics toolkit.
[64] Lipinski CA. Lead- and drug-like compounds: the rule-of-five revolution. *Drug Discov Today Technol.* 2004;1(4):337–341. doi:10.1016/j.ddtec.2004.11.007.
[65] Cereto-Massagué A, Ojeda MJ, Valls C, Mulero M, Pujadas G, Garcia-Vallvé S. Molecular fingerprint similarity search in virtual screening. *Methods.*2015;71:58–63. doi:10.1016/j.ymeth.2014.08.005.
[66] Liu X, et al. CB-Dock: a web server for cavity detection-guided protein–ligand blind docking. *Acta Pharmacol Sin.* 2020;10(7):1441–1445.
[67] Liu X, et al. CB-Dock2: improved protein–ligand blind docking by integrating cavity detection and template fitting. *Sci Rep.* 2022;12:(article number).

[68] Forli S, Huey R, Pique ME, Sanner MF, Goodsell DS, Olson AJ. Computational protein–ligand docking and virtual drug screening with the AutoDock suite. *Nat Protoc.* 2016;11(5):905–919.
[69] Trott O, Olson AJ. AutoDock Vina: improving the speed and accuracy of docking with a new scoring function. *J Comput Chem.* 2010;31(2):455–461.
[70] Berman HM, Westbrook J, Feng Z, et al. The Protein Data Bank. *Nucleic Acids Res.* 2000;28(1):235–242.
[71] Hollingsworth SA, Dror RO. Molecular dynamics simulation for all. *Neuron.* 2018;99(6):1129–1143.
[72] Kitchen DB, et al. Docking and scoring in virtual screening for drug discovery: methods and applications. *Nat Rev Drug Discov.* 2004;3(11):935–949.
[73] Morris GM, Huey R, Lindstrom W, et al. AutoDock4 and AutoDockTools4: automated docking with selective receptor flexibility. *J Comput Chem.* 2009;30(16):2785–2791.
[74] Liu X, Wang W, Liu P, Lei T, Chen S, Chen Y, et al. CB-Dock: a web server for cavity detection-guided protein–ligand blind docking. *Acta Pharmacol Sin.*2020;41:138–144. doi:10.1038/s41401-019-0228-6.
[75] Liu X, Li H, Wang W, Li D, Chen Y. CB-Dock2: improved protein–ligand blind docking by integrating cavity detection and template fitting. *Sci Rep.*2022;12:21105. doi:10.1038/s41598-022-25745-w.
[76] Trott O, Olson AJ. AutoDock Vina: improving the speed and accuracy of docking with a new scoring function. *J Comput Chem.* 2010;31(2):455–461. doi:10.1002/jcc.21334.
[77] Forli S, Huey R, Pique ME, Sanner MF, Goodsell DS, Olson AJ. Computational protein–ligand docking and virtual drug screening with the AutoDock suite. *Nat Protoc.*2016;11:905–919. doi:10.1038/nprot.2016.051.
[78] Trott O, Olson AJ. AutoDock Vina: improving the speed and accuracy of docking with a new scoring function. *J Comput Chem.* 2010;31(2):455–461. doi:10.1002/jcc.21334.
[79] Forli S, Huey R, Pique ME, Sanner MF, Goodsell DS, Olson AJ. Computational protein–ligand docking and virtual drug screening with the AutoDock suite. *Nat Protoc.*2016;11:905–919. doi:10.1038/nprot.2016.051.
[80] Liu X, Wang W, Liu P, Lei T, Chen S, Chen Y, et al. CB-Dock: a web server for cavity detection-guided protein–ligand blind docking. *Acta Pharmacol Sin.*2020;41:138–144. doi:10.1038/s41401-019-0228-6.
[81] Morris GM, Huey R, Lindstrom W, Sanner MF, Belew RK, Goodsell DS, et al. AutoDock4 and AutoDockTools4: automated docking with selective receptor flexibility. *J Comput Chem.* 2009;30(16):2785–2791. doi:10.1002/jcc.21256.
[82] Yuriev E, Ramsland PA. Latest developments in molecular docking: 2010–2011 in review. *J Mol Recognit.* 2013;26(5):215–239. doi:10.1002/jmr.2266.
[83] Trott O, Olson AJ. AutoDock Vina: improving the speed and accuracy of docking with a new scoring function. *J Comput Chem.* 2010;31(2):455–461. doi:10.1002/jcc.21334.
[84] Morris GM, Huey R, Lindstrom W, Sanner MF, Belew RK, Goodsell DS, et al. AutoDock4 and AutoDockTools4: automated docking with selective receptor flexibility. *J Comput Chem.* 2009;30(16):2785–2791. doi:10.1002/jcc.21256.
[85] Forli S, Huey R, Pique ME, Sanner MF, Goodsell DS, Olson AJ. Computational protein–ligand docking and virtual drug screening with the AutoDock suite. *Nat Protoc.*2016;11:905–919. doi:10.1038/nprot.2016.051.
[86] Yuriev E, Ramsland PA. Latest developments in molecular docking: 2010–2011 in review. *J Mol Recognit.* 2013;26(5):215–239. doi:10.1002/jmr.2266.
[87] Meng X-Y, Zhang H-X, Mezei M, Cui M. Molecular docking: a powerful approach for structure-based drug discovery. *Curr Comput Aided Drug Des.* 2011;7(2):146–157. doi:10.2174/157340911795677602.
[88] Kitchen DB, Decornez H, Furr JR, Bajorath J. Docking and scoring in virtual screening for drug discovery: methods and applications. *Nat Rev Drug Discov.* 2004;3(11):935–949. doi:10.1038/nrd1549.
[89] Sousa SF, Fernandes PA, Ramos MJ. Protein–ligand docking: current status and future challenges. *Proteins.* 2006;65(1):15–26. doi:10.1002/prot.21082.

[90] Hollingsworth SA, Dror RO. Molecular dynamics simulation for all. *Neuron.* 2018;99(6):1129–1143. doi:10.1016/j.neuron.2018.08.011.
[91] De Vivo M, Masetti M, Bottegoni G, Cavalli A. Role of molecular dynamics and related methods in drug discovery. *J Med Chem.* 2016;59(9):4035–4061. doi:10.1021/acs.jmedchem.5b01684.
[92] Gajewski M, Dominiak P, Gawor M, Cieplak P. Molecular dynamics simulations of protein–ligand complexes: a review. *BiochimBiophys Acta Gen Subj.* 2020;1864(12):129644. doi:10.1016/j.bbagen.2020.129644.
[93] Karplus M, McCammon JA. Molecular dynamics simulations of biomolecules. *Nat Struct Biol.* 2002;9(9):646–652. doi:10.1038/nsb0902-646.
[94] Hair JF, Black WC, Babin BJ, Anderson RE. *Multivariate Data Analysis.* 7th ed. Harlow: Pearson; 2014.
[95] Ritchie DW. Recent progress and future directions in protein–ligand docking. *Curr Protein Pept Sci.* 2008;9(5):463–480. doi:10.2174/138920308786786706.
[96] Willett P. Similarity-based virtual screening using 2D fingerprints. *Drug Discov Today.* 2006;11(23–24):1046–1053. doi:10.1016/j.drudis.2006.10.005.
[97] Tropsha A. Best practices for QSAR model development, validation, and exploitation. *Mol Inform.* 2010;29(6–7):476–488. doi:10.1002/minf.201000061.
[98] Landrum G. RDKit: Open-source cheminformatics. Version 2023.03.1. [Internet]. 2023 [cited 2026 Jan 12].
[99] Hunter JD. Matplotlib: A 2D graphics environment. *Comput Sci Eng.* 2007;9(3):90–95. doi:10.1109/MCSE.2007.55.
[100] McKinney W. *Python for Data Analysis: Data Wrangling with Pandas, NumPy, and IPython.* 2nd ed. Sebastopol: O'Reilly Media; 2017.
[101] Oliphant TE. Python for scientific computing. *Comput Sci Eng.* 2007;9(3):10–20. doi:10.1109/MCSE.2007.58.
[102] Walt S van der, Colbert SC, Varoquaux G. The NumPy array: a structure for efficient numerical computation. *Comput Sci Eng.* 2011;13(2):22–30. doi:10.1109/MCSE.2011.37.